

## A LASER HEATER FOR CLARA

S. Spampinati, University of Liverpool and The Cockcroft Institute, Warrington, Cheshire, U.K.  
B.D.Muratori, N.R. Thompson, P.H.Williams, ASTeC, Daresbury Laboratory, Warrington,  
Cheshire, U.K.

### Abstract

CLARA is a new FEL test facility, being developed at STFC Daresbury Laboratory in UK, based on a high brightness electron linac. The electron beam of CLARA can potentially be affected by the longitudinal microbunching instability leading to a degradation of the beam quality. The inclusion of a laser heater in the linac design can allow control of the microbunching instability, the study of microbunching and deliberate increase of the final energy spread to study energy spread requirements of the FEL schemes tested at CLARA. We present the initial design and layout of the laser heater system for CLARA and its expected performance.

### INTRODUCTION

CLARA (Compact Linear Accelerator for Research and Applications) is a proposed 250MeV, 100-400nm FEL test facility at Daresbury Laboratory [1]. The purpose of CLARA is to test, explore and ultimately validate new schemes for FEL light generation in areas such as ultra-short pulse generation, temporal coherence and pulse-tailoring. The accelerator itself will consist of 4 S-Band normal conducting linear accelerators with a medium-energy variable bunch compression scheme, feeding into a flexible arrangement of FEL modulators and radiators. For seeding purposes the accelerator includes a pre-FEL dogleg where modulated laser light can be introduced. The accelerator will be driven by a high rep-rate RF photo-cathode S-Band electron gun, operating in single bunch mode at up-to 100Hz, and with bunch charges up to 250pC. Peak currents at the FEL are expected to be in the 500A range running the linac with the magnetic bunch compressor. An increased current in the 1-2 KA range can be obtained through the use of a velocity-bunching scheme in the first two linac structures [2]. The CLARA linac is potentially affected by the longitudinal microbunching instability (MBI) [3-5], as are other accelerators that drive high gain free electron laser (FEL) facilities [6,7], that produce short wavelength ( $\sim 1-5\mu\text{m}$ ) energy and current modulations. These can both degrade the FEL spectrum and reduce the power by increasing the slice energy spread. This instability is presumed to start at the photoinjector exit growing from a pure density modulation caused by shot noise and/or unwanted modulations in the photoinjector laser temporal profile. As the electron beam travels along the linac to reach the first bunch compressor (BC1), the density modulation leads to an energy modulation via longitudinal space charge. The resultant energy modulations are then transformed into higher density modulations by the bunch compressor. The increased current non-uniformity leads

to further energy modulations along the rest of the linac. Coherent synchrotron radiation in the bunch compressor can further enhance these energy and density modulations [8,9]. The main solution to prevent MBI, used in several FEL facilities, is the laser heater (LH) [10,11].

A laser heater consists of a short, planar undulator located in a magnetic chicane where an external infrared laser pulse is superimposed temporally and spatially over the electron beam. The electron-laser interaction within the undulator produces an energy modulation on a longitudinal scale length corresponding to the laser wavelength.

The second half of the LH chicane smears the energy modulation in time, leaving the beam with an almost pure incoherent energy spread. This controllable incoherent energy spread suppresses further MBI growth via energy Landau damping in the bunch compressor. A layout of a laser heater is shown in Fig. 1.

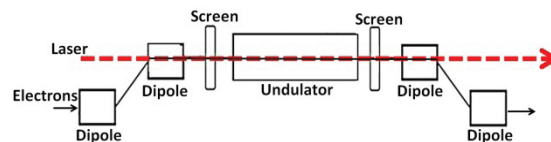


Figure 1: Laser heater layout.

The presence of the laser heater in a test facility like CLARA could be exploited to study further some less explored aspects of MBI such as the microbunching induced by the laser heater chicane and the MB competition between different sections of the accelerator [12].

The laser heater can also be used to modulate the electron beam energy spread to control the FEL temporal and spectral properties [13] or to deliberately increase of the final energy spread to study energy spread requirements of the FEL schemes tested at CLARA. The laser heater chicane could be also used to implement the diagnostics presented in [14]. These are all possible experiments of relevance to future FEL facilities. Consequently a space for a laser heater system has been left in the linac layout. Due to space constraints and to the necessity to avoid long strait sections at low energy the more convenient location for the laser heater is just before the bunch compressor at a beam energy of 125-210 MeV. In this case the beam present a significant energy chirp ( $\sim 2\%$ ) and this is a difference respect to other facility [6,7]. The effect of the chirp on the laser heater will be analysed.

After the first acceleration stage a set of 4 quadrupoles allows matching of the optical functions into the laser heater chicane and 4 additional quadrupoles follow the

LH chicane to control the matching in the bunch compressor region. The values of the basic parameters of the electron beam in the laser heater region are reported in table 1.

Table 1: Electron Beam Parameters

Parameter	Value	Unit
Energy	125-210	MeV
Pulse duration	4-6	ps
Chirp	<2	%
Slice energy spread	3	keV
Emittance	0.6	mm·μrad
$\sigma_x, \sigma_y$	220	μm
$\sigma'_x, \sigma'_y$	11	μrad

## SYSTEM DESCRIPTION

The laser pulse used for the laser heater could be a small portion of the photocathode infrared drive laser picked up just before the harmonic up-conversion to UV, similar to systems installed in other facilities [6,7]. The laser pulse has to be stretched to be 2-3 times longer than the electron beam. Pulse energy of 150-200 μJ should be available.

The chicane has to provide enough room for the insertion of the electron beam on the laser path and an effective smearing of the time energy correlation induced by the laser. The  $R_{56}$  and the dispersion of the chicane have to be kept small possible as the beam acquires a chirp.

A possible design of the chicane has bending angles of 4.5 degrees, a separation between the first and the second dipole as between the third and fourth dipole of 30 cm, a dipole length of 10 cm and a total chicane length of 2,0-2,7 m. The maximum dispersion (in the center of the chicane) and the  $R_{56}$  of this chicane are 4.5 mm and 31 mm, respectively. This design provides a horizontal trajectory bump of 3.1 cm, sufficient to overlap the laser and the electron beam, and a good smearing of the energy modulation at the laser wavelength. This smearing occurs because the path length, from the chicane center (where the energy modulation is induced) to the chicane end, depends on the electron's horizontal divergence through the transport matrix element  $R_{52}$ . Therefore, the energy/position correlation, induced in the undulator, is smeared if the following relation is satisfied

$$\left| R_{52} \cdot \sigma_x \right| = \left| \eta_{\max} \cdot \sigma_x \right| > \frac{\gamma_r}{2\pi} \quad (1)$$

with a dispersion value of 31 mm and an angular spread of 11 μrad, the rms temporal smearing is 340 nm, which

is large compared to the reduced wavelength of 127 nm. Thus the 800 nm energy correlation is efficiently smeared.

The  $R_{56}$  of the laser heater chicane is around ten times smaller than the  $R_{56}$  of the bunch compressor chicane (photoinjector accelerates approximately on crest), the laser heater chicane produces a small bunch compression (<10%) This effect is not critical for the subsequent compression. The laser heater undulator is a variable gap planar undulator composed of 7 periods of 5.5 cm each. This undulator is resonant with the 800 nm laser at beam energy of 150 MeV for a value of the strength parameter  $K$  equal to 1.2. Figure 2 shows the resonant  $K$  value as function of the beam energy. The minimum undulator gap required to have the resonance at 210 MeV is 24 mm (considering a remanent field of 1.25 T).

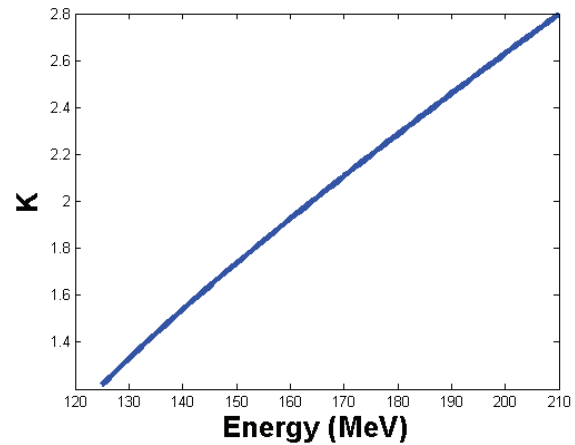


Figure 2: Resonant undulator factor  $K$  versus beam energy.

The basic parameters of laser, chicane and undulator are reported in table 2. It is possible to estimate the energy spread induced in the beam by the laser heater using the following formulas [4]

$$\sigma_\varepsilon = \int_0^{L_U} \sqrt{\frac{\sigma_r^2(x)}{2 \cdot (\sigma_x^2 + \sigma_r^2(x))}} \sqrt{\frac{P_L}{P_0} \cdot \frac{K}{\gamma_0} \frac{1}{\sigma_r(x)}} m_0 c^2 [JJ] dx \quad (2)$$

where  $\sigma_x$  and  $\sigma_r$  are the rms transverse dimension of the electron and the laser beam, respectively,  $L_U$  is the undulator length,  $\gamma_0$  is the electron beam mean energy,  $P_L$  is the laser beam peak power,  $JJ$  is the undulator coupling factor [15] and  $P_0 = 8.9$  GW. The integration is on the longitudinal undulator coordinate. Figure 3 reproduces the induced energy spread as function of the laser energy considering a laser pulse length (FWHM) of 15 ps.

Table 2: Laser Heater Parameters

Parameter	Value	Unit
Wavelength	800	nm
$\sigma_x, \sigma_y$	220	$\mu\text{m}$
Laser pulse duration	10-15	ps
Laser max energy	150-200	$\mu\text{J}$
Bending angle	4.5	$^\circ$
Dipole length	10	cm
Drift 1-2(3-4) dipoles	30	cm
Undulator period	5.5	cm
Number of period	7	

Figure 3 reproduces the induced energy spread as function of the laser energy considering a laser pulse length (FWHM) of 15 ps.

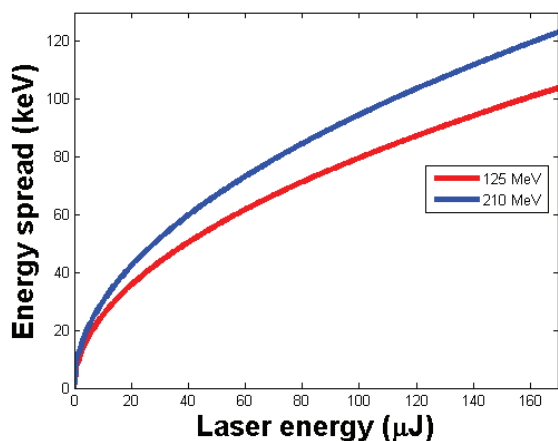


Figure 3: Slice energy spread versus Laser power.

Pulse energy of 0.3-0.5  $\mu\text{J}$  is required to have an energy spread of 5-10 keV and then suppress the microbunching. An Energy spread higher than this suppression threshold is amplified by bunch compression as the area of the longitudinal phase space is conserved. The maximum energy spread delivered at the end of the linac, is for a compression factor 5-8, 500-800 keV, equivalent to a relative energy spread of 0.2% -0.35% at 250 MeV. This level of relative energy spread is comparable with the Pierce parameter [1,16] of CLARA and so is sufficient to affect the FEL process.

The level of heating provided by the system described is enough to study and suppress microbunching and to study the energy spread requirement of several FEL schemes tested at CLARA. Modulation of this large energy spread done with the technique described in [13]

can modify the spectral and temporal properties of the FEL pulse.

Two CROMOX ( $\text{Al}_2\text{O}_3:\text{Cr}$ ) screens, one on each side of the undulator, allow imaging both the laser beam and the electron beam in order to superimpose them transversely.

### SIMULATIONS

Simulations including the beam energy modulation in the laser heater undulator and the transverse dynamic in the laser heater chicane have been performed with the code ELEGANT [17] to test the performance of system described above. A first set of simulations have been performed using the full beam distribution to study the effect of the energy chirp on the energy spread induced by the laser heater. 2M macro-particles have been used in these simulations. The phase space of the heated beam at the exit of the chicane is reproduced in fig. 4. The electron beam has a chirp of 2% and the laser pulse has a length (FWHM) of 15 ps and energy of 20  $\mu\text{J}$ .

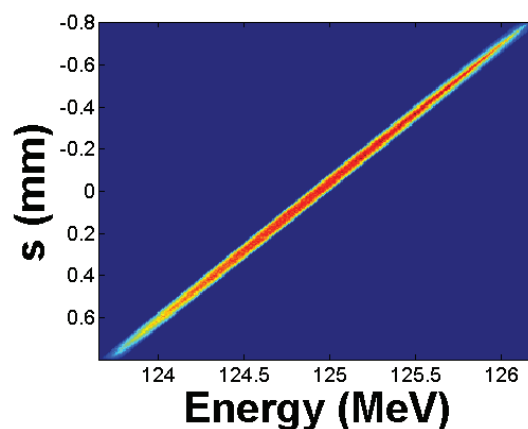


Figure 4: Electron beam phase space after the laser heater.

The slice energy spread along the beam is reproduced in fig 5. We see that the variation of the beam heating is about 20% on the total beam length and correspond to what is found experimentally in other working laser heaters where the beam has a more flat energy profile in the laser heater [7]. This seems to be a good level of uniformity.

Other simulations have been performed using only a small central part of the beam to study the smearing of the energy modulation in the second part of the chicane. Figure 6a and 6b reproduce the phase space after the laser heater undulator and after the chicane. In this case the pulse energy is 0.3  $\mu\text{J}$ . The energy spread induced in this case is 6 keV and should be close to the value that suppresses efficiently the microbunching instability. 2M macro-particles have been used in these simulations. We see that the energy correlation is removed by the beam dynamic in the second part of the chicane. We can see in fig 6c that the correlation is now transferred in the t-xp plane. This correlation can restore a microbunching on the laser wavelengths along the beam line in the point in which the transport element from the center of the chicane

goes to 0. This transient microbunching can induce a certain level of energy spread [6]. This effect is strongly depended by the optics from the laser heater to the bunch compressor [6,12]. In the bunch compressor any correlation is removed by the strong  $R_{56}$  of the chicane. The optics from the laser heater to the bunch compressor should avoid waist in the  $x$  plane between the laser heater and the bunch compressor.

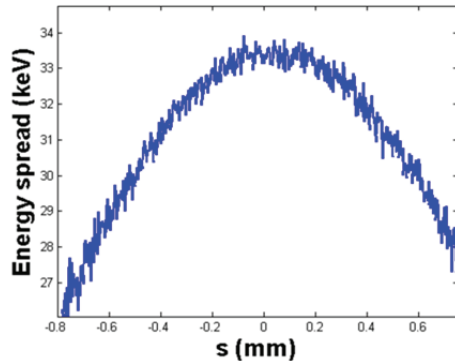


Figure 5: Energy spread after the laser heater.

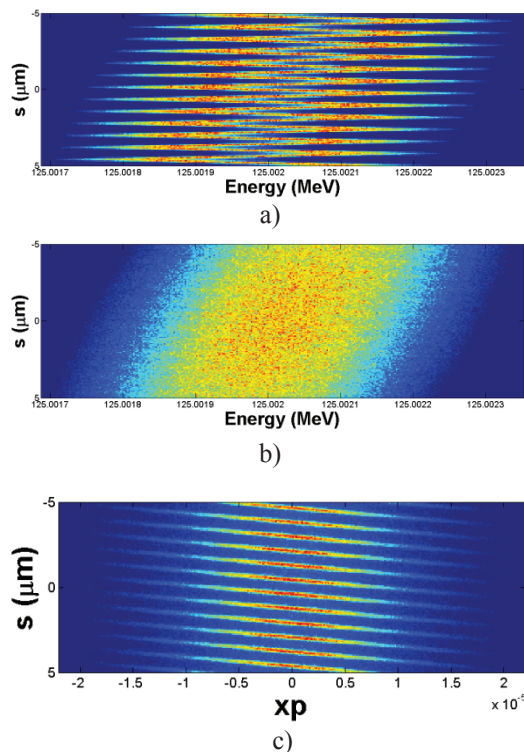


Figure 6: a) Phase space in the center of the chicane after the undulator. b) Phase space after the chicane. c)  $t$ - $xp$  correlation after the chicane.

## CONCLUSION

We have presented a possible design of the CLARA laser heater and simulations of its operation. The level of heating provided by this design is enough to study and suppress microbunching and to study the energy spread requirement of the several FEL schemes tested at CLARA. The homogeneity of the heating along the beam is good despite the presence of the chirp used to compress the beam.

## REFERENCES

- [1] J. A. Clarke et al, JINST 9 T05001 (2014).
- [2] M. Ferrario et al. Phys. Rev. Lett. 104, 054801 (2010).
- [3] E.L. Saldin, E.A. Schneidmiller, and M.V. Yurkov, Nucl. Instrum. Methods Phys. Res. A 490, 1(2002).
- [4] T. Shaftan and Z. Huang, Phys. Rev. ST Accel. Beams 7, 080702 (2004).
- [5] S. Seletskiy et al. Phys. Rev. ST Accel. Beams 14, 110701 (2011).
- [6] Z. Huang et al., Phys. Rev. ST Accel. Beams 13, 020703 (2010).
- [7] S. Spampinati et al., Phys. Rev. ST Accel. Beams 17, 120705 (2014).
- [8] T. Limberg, P. Piot, and E. A. Schneidmiller, Nucl. Instrum. Methods Phys. Res., Sect. A 475, 353 (2001).
- [9] S. Heifets, S. Stupakov, and S. Krinsky, Phys. Rev. ST Accel. Beams 5, 064401 (2002).
- [10] E. L. Saldin, E. A. Schneidmiller, and M. V. Yurkov, Nucl. Instrum. Methods Phys. Res., Sect. A 528, 355 (2004).
- [11] Z. Huang, M. Borland, P. Emma, J. Wu, C. Limborg, G. Stupakov, and J. Welch, Phys. Rev. ST Accel. Beams 7, 074401 (2004).
- [12] D. Ratner et al Phys. Rev. ST Accel. Beams 18, 030704 (2015).
- [13] E. Roussel et al. "Influence of a non-uniform longitudinal heating brightness electron beams for FEL", proceedings of IPAC 2015.
- [14] R. Fiorito et al., Phys. Rev. ST Accel. Beams 17, 122803 (2014).
- [15] W. B. Colson, IEEE J. Quantum Electron. 17, 1417 (1981).
- [16] R. Bonifacio, C. Pellegrini, and L. Narducci, Opt. Commun. 50, 373 (1984).
- [17] M. Borland, ANL/APS Report No. LS-287 (2000).